

The dipole corrector magnets for the FFAG beam line of the CBETA accelerator

N. Tsoupas

August 2019

Collider Accelerator Department
Brookhaven National Laboratory

U.S. Department of Energy

USDOE Office of Science (SC), Nuclear Physics (NP) (SC-26)

Notice: This technical note has been authored by employees of Brookhaven Science Associates, LLC under Contract No. DE-SC0012704 with the U.S. Department of Energy. The publisher by accepting the technical note for publication acknowledges that the United States Government retains a non-exclusive, paid-up, irrevocable, world-wide license to publish or reproduce the published form of this technical note, or allow others to do so, for United States Government purposes.

DISCLAIMER

This report was prepared as an account of work sponsored by an agency of the United States Government. Neither the United States Government nor any agency thereof, nor any of their employees, nor any of their contractors, subcontractors, or their employees, makes any warranty, express or implied, or assumes any legal liability or responsibility for the accuracy, completeness, or any third party's use or the results of such use of any information, apparatus, product, or process disclosed, or represents that its use would not infringe privately owned rights. Reference herein to any specific commercial product, process, or service by trade name, trademark, manufacturer, or otherwise, does not necessarily constitute or imply its endorsement, recommendation, or favoring by the United States Government or any agency thereof or its contractors or subcontractors. The views and opinions of authors expressed herein do not necessarily state or reflect those of the United States Government or any agency thereof.

1 The dipole corrector magnets for the FFAG beam line
2 of the CBETA accelerator¹

3 N. Tsoupas², J. S. Berg, S. Brooks, A. Jain, F. Méot, G. Mahler,
4 S. Trabocchi, D. Trbojevic, J. Tuozzolo

5 *Brookhaven National Laboratory, Collider-Accelerator Department, Upton, LI, NY*
6 *11973, USA*

7 **Abstract**

8 The Cornell Brookhaven Experimental Test Accelerator (CBETA) [1] is a
9 novel, and the first of its kind electron accelerator to combine two remark-
10 able concepts, the Energy Recovery Linac (ERL) [2] and the Fixed Field
11 Alternating Gradient (FFAG) concept [3]. The accelerator has been built
12 at Cornell University in collaboration with Brookhaven National Laboratory
13 (BNL) and it is at its commissioning stage. The FFAG beam line consist of
14 two arcs sections and a straight section, with all sections comprised of single
15 cells, each cell made of two Halbach type of magnets. The cell in the arcs
16 consists of one focusing quadrupole and a combined function magnet which
17 is comprised of a dipole and a defocusing quadrupole multipole. The cells in
18 the straight section consist of a focusing and a defocusing quadrupoles. Each
19 focusing quadrupole has a window-frame dipole corrector magnet generating
20 vertical dipole field and the other magnet has a corrector generating hori-
21 zontal dipole field. This technical note reports on the mechanical design and
22 the electromagnetic properties of these window frame corrector magnets.

23 *Keywords:* FFAG, ERL

24 **1. Introduction**

25 The CBETA electron accelerator [1] is unique of its kind to combine
26 two remarkable concepts, the Energy Recovery Linac (ERL) concept and the
27 Fixed Field Alternating Gradient (FFAG) concept. Fig. 1 is a top view of the
28 CBETA accelerator. A 6 MeV electron bunch generated from the injector
29 (IN) shown in Fig. 1 is injected to the ERL (LA) to increase the kinetic

¹Work supported by the US Department of Energy and NYSERDA

²tsoupas@bnl.gov

30 energy of the electron bunch by 36 MeV and subsequently enters the “42
 31 MeV” line of the four-line splitter section (SX) of the accelerator.

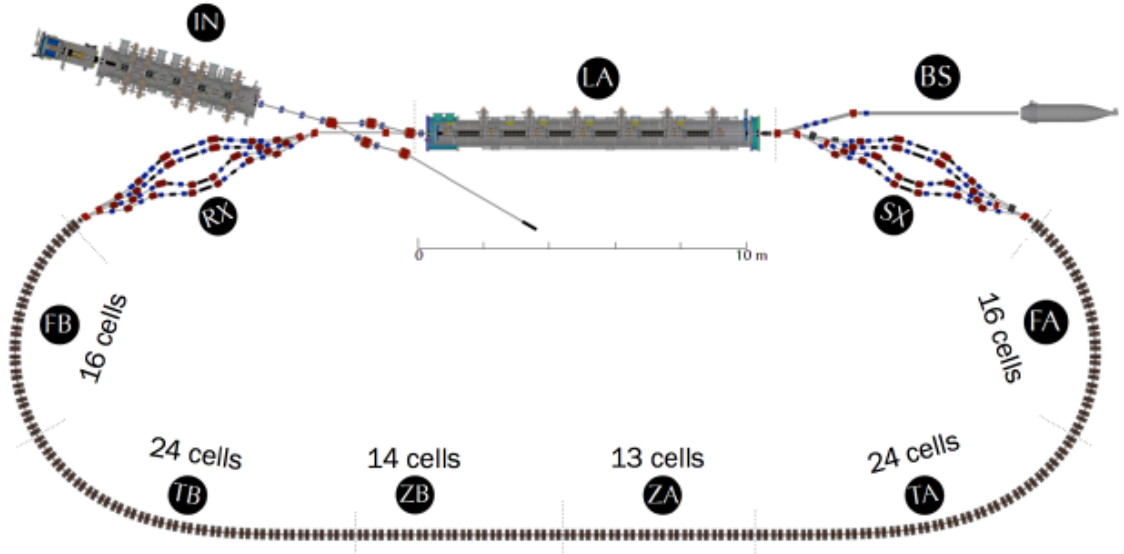


Figure 1: Layout of the CBETA accelerator. The section labeled (IN) is the 6 MeV electron injector into the CBETA accelerator. The section labeled (LA) is the ERL, the sections labeled (FA), (TA), (ZA), (ZB), (TB), and (FB) are the FFAG sections which accommodate four recirculating electron bunches in the energy range from 42 MeV to 150 MeV. The sections (SX) and (RX) are the splitter and combiner sections respectively each comprised of four lines to transport the electron bunches with energies 42, 78, 114, and 150 MeV respectively.

32 The 42 MeV beam line of the splitter (SX) transports the electron bunches
 33 to the FFAG-sections (FA, TA, ZA, ZB, TB, EB) and the combiner (RX)
 34 section, recirculate the bunches to the entrance of the ERL for the bunches
 35 to receive an additional 36 MeV at the exit of the ERL. The bunches attain
 36 their final energy of 150 MeV after two additional recirculations in the FFAG.
 37 Subsequently, by changing the path length of the 150 MeV bunch, the phase
 38 of the electron bunches with respect to the RF accelerating field of the ERL
 39 changes by 180° and the energy of the electron bunches is reduced by 36
 40 MeV each time the bunches transverse the the ERL, for their energy to be
 41 reduced to 6 MeV after four recirculations through the ERL. The 6 MeV
 42 electron bunches are dumped in the designated electron dump (BS). It is
 43 for the remarkable property of the FFAG that electron bunches with energy
 44 range from 42 MeV to 150 MeV can be transported by the single FFAG

45 transport line which consists of the sections (FA), (TA), (ZA), (ZB), (TB),
 46 and (FB) shown in Fig. 1.
 47 The FFAG transport line consists of 107 cells each comprised of two Halbach
 48 type permanent magnets. The cell in the arcs (FA), (TA), (TB), and (FB)
 49 consist of a focusing quadrupole (QF) and a combined function magnet (BD)
 50 which is a combination of a dipole multipole, and a defocusing quadrupole
 51 multipole. Each cell in the straight section (ZA), (ZB), consist of a focusing
 52 quadrupole (QF) and a defocusing quadrupole. Fig. 2 is a perspective view of
 53 three consecutive FFAG arc-cells of the CBETA. Each QF and DB magnet of the
 54 cell has a window frame iron core with a coil generating a vertical dipole
 55 field for the QF magnet and an horizontal dipole field for the BD magnet.
 These window frame magnets act as dipole corrector magnets. This paper

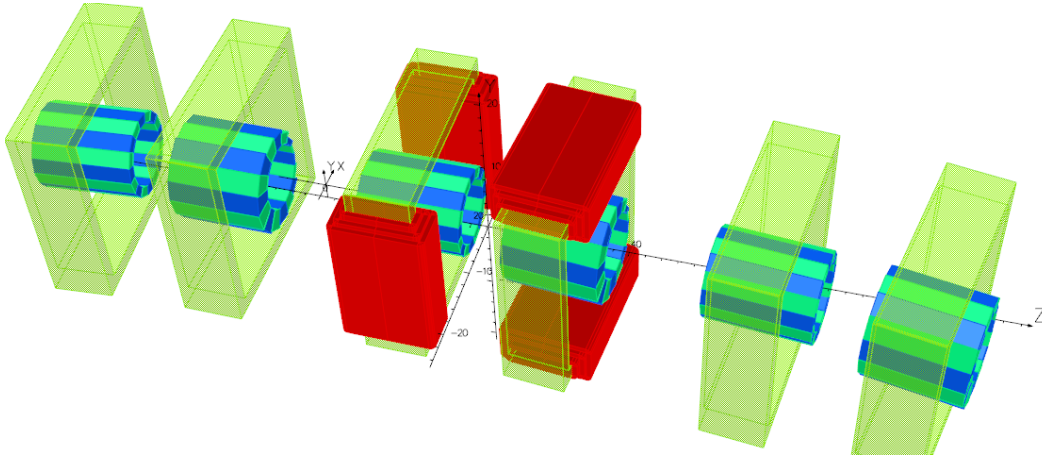


Figure 2: A perspective view of three consecutive cells of the FFAG arcs. Each cell consists of two magnets, one of a focusing quadrupole (QF) and one of a combine function (BD) with dipole and quadrupole multipoles. Each magnet has a window frame magnet acting as a corrector.

56
 57 provides information on the mechanical and the electromagnetic properties
 58 of the window frame magnet. The effect of the dipole corrector magnet on
 59 the magnetic multipoles of a Halbach magnet is discussed and calculations
 60 and experimental results are presented. The extend of the dipole field of each
 61 corrector magnet on the neighboring magnets is also studied and presented.

62 **2. Description of the mechanical design of the window frame mag-**
 63 **net**

64 Mechanical drawings of the window frame magnet are showing in Figs. 3
 and 4. The dimensions in the drawings are in inches. Table 1 lists the

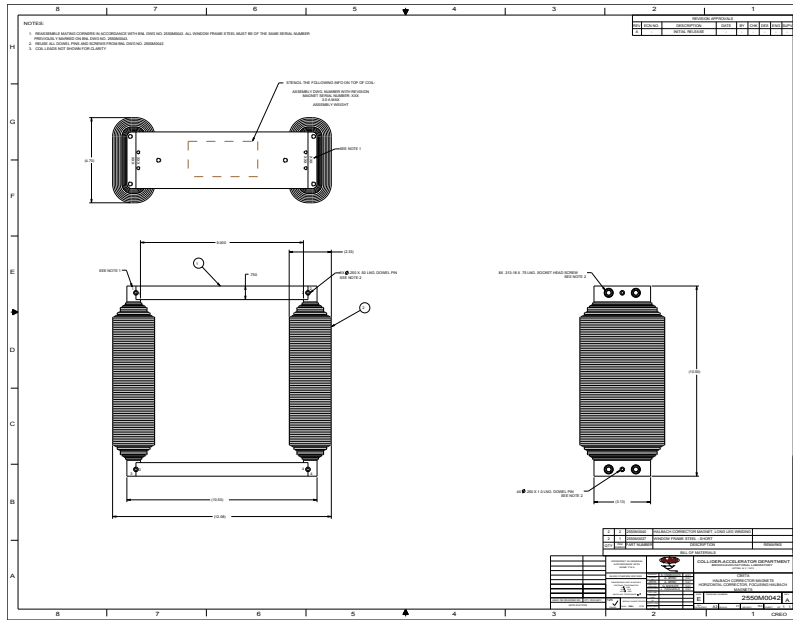


Figure 3: A mechanical drawing of the corrector showing the dimensions in inches of the iron core of the window frame magnet.

65
 66 dimensions in units of cm of the square window frame iron core. The thickness
 67 (label “Thick” in Table 1) of the iron frame has been chosen for the iron not
 68 to saturate when the corrector is excited at its maximum field. The inner
 69 width (W) and height (H) of the frame have been chosen to allow space for
 70 the placement of an aluminum block shown in Fig. 5 around the magnet for
 71 keeping the temperature of the permanent magnet constant. The length of
 72 the iron frame has been chosen for the coil of the corrector magnet not to
 73 extend into the drift space between the Halbach type of magnets.

74 *2.1. The coil of the dipole corrector magnet*

75 The constrain on the maximum field generated by the corrector and the
 76 optimum power supply to be used to power the magnet, defines the AWG

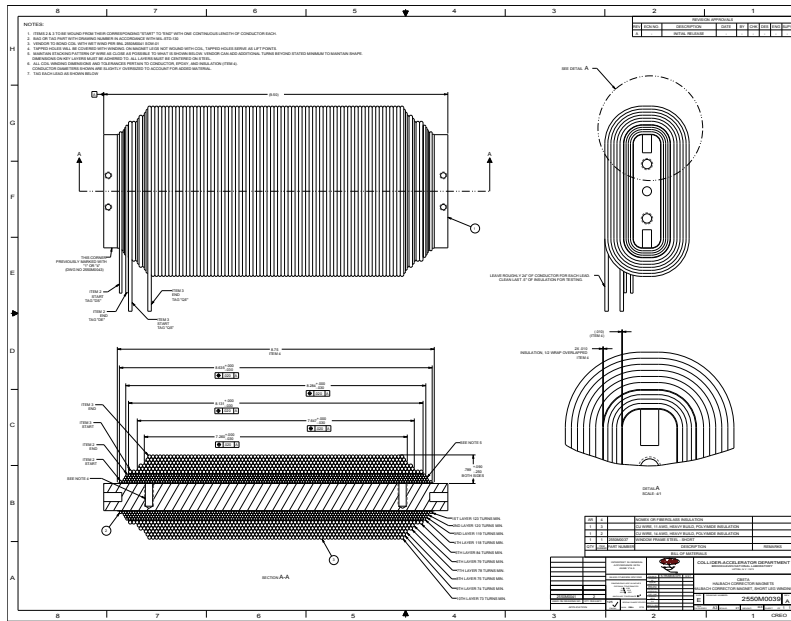


Figure 4: A drawing of the window frame magnet showing the number of copper-wire-turns wound in one of the sides of the frame to make the coils. Dimensions in the drawing are in inches. The maximum current running through the wire of the coils is 2.29 A

77 gauge and the turns of the conductors which make the magnet's air cooled
 78 coils.

79 Fig. 4 is a another drawing of the magnet which shows that there are
 80 10 layers of copper conductors for each coil and lists the number of turns of
 81 the copper conductors per layer. The first four inner layers of each coil are
 82 made of copper conductor gauge 14 and the rest six layers of copper conduc-
 83 tor gauge 11. Both wire conductors have heavy built polyimide insulation.
 84 Initially the corrector magnet was designed to generate a dipole field by con-
 85 necting in series the coil made of the four inner layers to that of the opposite
 86 side of the frame, and also generate a quadrupole field by "appropriately"
 87 connecting the outer-six-layers-coil of one side, with the corresponding coil
 88 placed on the other three sides of the frame. Table 2 lists the number of
 89 layers and the turns per layer wound around each side of the iron window
 90 frame. The gauge of the copper wire conductors is also listed in Table 2. For
 91 completion we introduce Table 3 which lists the inductance of the window
 92 frame magnet when various combinations of the coils are used to generate
 93 Normal and Skew dipoles and Normal quadrupole. In Table 3 the meaning of

94 symbols are: N (Normal) S (Skew) V (Vertical) H (Horizontal). To generate
 95 a Skew quadrupole the window frame magnet should be rotated by 45° . In
 96 this case four coils, one in each side of the window frame magnet have to be
 97 used to generate either normal or skew dipole or a combination of both.
 98 APPENDIX B describes possible coil-connection of a window frame magnet
 99 that generates dipole and quadrupole fields as well as a combination of of
 100 both multipoles as described above. In addition APPENDIX B describes
 101 possible use of floating power supplies to generate a combination of Normal
 102 Dipole, Skew Dipole, and Normal Quadrupole multipoles. In the CBETA
 103 setup the coil made of wire gauge 14 is connected in series to that of gauge
 104 11 and this combined coil is connected in series with the coil on the opposite
 105 side of the window frame to make a dipole corrector, with the maximum
 106 current running through the coil's conductors at 2.29 A. The coils which
 107 generate the vertical dipole field (Horizontal-corrector) are placed on the
 108 vertical sides of the window frame and those which generate the horizontal
 109 field (Vertical-correctors) are placed on the horizontal sides of the window
 110 frame.

Table 1: Dimensions of the square window frame iron of the corrector magnet.

Length	Inner(W/H)	Out(W/H)	Thick
[cm]	[cm]	[cm]	[cm]
7.95	22.86	26.67	1.905

Table 2: The number of copper-wire turns in each of the layers of the coils. The wire gauge of the layers 1 to 4 is AWG=14 the rest layers have wire gauge of AWG=11

Layer #	1	2	3	4	5	6	7	8	9	10	Total turns
# of turns	123	120	119	118	84	79	78	75	74	73	914
Wire AWG	14	14	14	14	11	11	11	11	11	11	

Res. [Ω]	Induct. [H]	I_{max} [A]
2.61	0.680	2.29

Table 3: Inductance of the window frame magnet based on the coils used to generate a combination of dipole and quadrupole corrector

Multipole	Coils	Layers/side	Turns/side	Inductance [H]
N-Dipole	V-Side	1 to 4	480	0.192
N+S-Dipole	V+H-Side	1 to 4	480	0.377
N-Dipole	V-Side	1 to 10	914	0.680
N-Quad	V+H-Side	5 to 10	434	0.129
N+S-Dip N-Quad	V+H-Side	1-4 5-10	480 434	0.504

111 3. The electromagnetic properties of the dipole corrector magnet

112 The OPERA computer code [2] was used to calculate the electromagnetic
 113 properties of the window frame dipole corrector magnet. Because the cross
 114 section of the magnet's iron is well defined (window frame) there was no need
 115 to shape the magnet's pole faces, therefore only 3D calculations were per-
 116 formed to calculate the multipoles of the magnet. These multipoles include
 117 the effect (interference) of the iron frames of the neighboring magnets. Fig. 6
 118 is a perspective view of the B_y field on a rectangular patch on the median
 119 plane. This B_y field is generated by the single window frame magnet with
 120 the coils as shown in Fig. 6. The 2D view of the B_y field shown in Fig. 6 is
 121 generated by the window frame magnet having the iron's permeability and
 122 the current in the conductors of the coils is 2.29 A. The rest of the window
 123 frames shown in the figure have permeability $\mu=1$. The extend of the B_y
 124 field in Fig. 6 has to be compared with the extend of the field generated by
 125 the same magnet but with the neighboring frames of the corrector magnets
 126 having the same permeability of the iron as the corrector magnet with the
 127 coils. The extend of the B_y field shown in Fig. 7 is less than that shown in
 128 Fig. 6 because the iron frames in Fig. 7 have the permeability of magnetic
 129 iron and act as field clamps.

130 Although Figs. 6 and 7 show some details of the dipole field generated
 131 by the window frame corrector magnet, like the existence of some sextupole
 132 component of the dipole field, a better way to view the variation of the
 133 B_y component of the field as a function of the z distance measured from the
 134 center of the corrector magnet is shown in Fig. 8. The rectangles on the figure
 135 are the iron frames of the corrector magnets. The black curve corresponds to

136 the B_y field with all the window frames having permeability $\mu=1$ except the
 137 window frame which generates the field that has the permeability of magnetic
 138 iron. The red curve corresponds to the B_y field with all the window frames
 139 having permeability of magnetic iron. Notice the red curve is not symmetric
 140 with respect to the center of the magnet at $z=0$, because the neighboring iron
 141 frames are not place symmetrically with the frame of the central magnet. An
 142 important information which can be used in beam optics calculations is the
 143 strength of the multipoles generated by the field of the corrector. These
 144 multipoles are generated by a Fourier expansion of the radial components of
 145 the field at a radius $R= 1$ cm and are plotted as a function of the the distance
 146 from the center of the corrector magnet in Fig. 9. The integrated strength of
 147 each multipole is shown in Table 4. The existance of a quadrupole multipole
 148 in a magnet with dipole symmetry is explained by the asymmetric placement
 149 of the neighboring window frame iron cores which affect the otherwise dipole
 150 symmetric field of the corrector. In Fig. 9 the values of the quadrupole and
 151 sextupole multipoles have been multiplied by 100 to be made visible in the
 152 plot. The integrated strength of the multipoles higher than sextupole is two
 153 order of magnitude lower then the sextupole strength. It is understood that
 154 the multipoles generated by the dipole corrector may be different along the
 155 four reference trajectories of the electron bunches, but simulation studies
 156 show that this difference is of second order effect.

Table 4: The integrated multipoles of the dipole corrector at a radius $R=1$ cm.

Dipole [Tm]	Quadrupole [Tm]	Sextupole [Tm]
2.1714×10^{-3}	1.94×10^{-6}	1.79×10^{-6}
Dipole [units]	Quadrupole [units]	Sextupole [units]
10000	8.9	8.2

157 **4. superposition of the dipole corrector field with the field of the** 158 **Halbach magnet**

159 Prior of deciding to manufacture and place the corrector magnets around
 160 the main Halbach magnets, magnetic field measurement were performed to

161 measure the effect of the dipole's corrector field on the main field of the
162 permanent magnet. Although it is clear that a permanent magnet is sat-
163 urated along the easy direction ($\mu=1$), therefore any external field will be
164 superimposed along this direction, it was not clear how a known external
165 field applied on a different direction will change the field of the permanent
166 magnet. Such an experimental study was conducted [3] and the results of
167 the measurements showed that the effect of the dipole correctors excited to
168 their maximum field on the FFAG main magnets is almost negligible. The
169 left picture in Fig. 10 shows the permanent magnet wedges which comprise
170 a modified quadrupole Halbach magnet and the window frame magnet sur-
171 rounding the Halbach magnet. The right picture in Fig. 10 is an expanded
172 view of the window frame magnet. The cylindrical pipe through the dipole
173 magnet is the rotating coil which measures the integrated multipoles of the
174 PM-Quad+WF-Dipole assembly. APPENDIX A presents the results of the
175 magnetic measurements performed by [3] and the conclusions.

176 **5. Appendix A: Superposition of Dipole field with the field of a** 177 **Permanent Magnet Quadrupole**

178 This section includes the results of the magnetic measurements performed
179 by [3].

180 Fig. 11 shows the effect of the bare WF yoke on the normal (left) and skew
181 (right) integrated multipoles of the PM quadrupole.

182 Fig. 12 shows the effect of the Horizontal Field Generated by the WF dipole
183 which is excited at its nominal current, on the normal (left) and skew (right)
184 integrated multipoles of the PM quadrupole.

185 Fig. 13 shows the effect of the Vertical field generated by the WF dipole on
186 the normal (left) and skew (right) integrated multipoles of the PM quadrupole.

187 Fig. 14 shows the effect of the Horizontal and Vertical fields generated by
188 the WF dipole on the normal (left) and skew (right) integrated multipoles of
189 the PM quadrupole.

190 Fig. 15 is the summary of the measurements as provided by [3].

191 **6. Appendix B: Generating a Dipole and a quadrupole field using**
192 **the same four coils of a WF magnet**

193 The main sections of this technical note is devoted in providing infor-
194 mation on the mechanical and electromagnetic properties of window frame
195 magnet which generates a normal dipole (vertical field) by exciting two coils
196 on the opposite vertical sides of the iron frame or generate a skew dipole
197 (horizontal field) by exciting two coils on the opposite horizontal sides of the
198 iron frame. This appendix discusses methods on how to connect coils of the
199 widow frame magnet to generate a normal quadrupole or a skew quadrupole
200 and combination of quadrupole field with dipole field. To cover as many
201 possibilities of quadrupole and dipole fields the subsections below start with
202 the most simple cases.

203 *6.1. Normal dipole only*

204 Details of generating a normal dipole was discussed in the main part of
205 this technical note and in this subsection a schematic figure is provided to
206 explain the connection of the coils of the window fram magnet. The picture
207 in Fig. 16 (a) is a cross section of WF magnet with two racetrack coils wound
208 around the vertical side to generate a normal dipole field. For simplicity in
209 all the text below this magnet will be represented by only the two inner
210 conductors of the coils as shown in Fig. 16 (c) with the outer conductors and
211 the WF iron omitted. Fig. 17 is a schematic diagram showing the connection
212 of the coils to generate a normal dipole field. Note that the top and bottom
213 coils are not connected to a power supply. The sense of the normal field
214 (pointing up or down) is adjusted by the polarity of the power supply.

215 *6.2. Skew dipole only*

216 To generate a skew dipole (horizontal field) the top and bottom coils
217 shown in Fig. 17 are used instead of the vertical coils. Otherwise the connec-
218 tion of the coils is identical to that of generating a normal field. The rotation
219 of the WF magnet, which generates normal dipole field, by 90° is equive-
220 lent to magnet which generates skew dipole field. At present the correction
221 magnets of the CBETA FFAG line are either normal or skew dipoles.

222 *6.3. Normal and skew dipoles of same strength and sense*

223 Fig. 18 is a schematic diagram for the wire connection of the coils of
224 the WF magnet which generates both normal and skew dipoles. If the coils

225 which generate normal field are identical to those which generate skew field,
226 the strength of the normal dipole is the same with that of the skew dipole.
227 Also if the of the normal field changes by changing the polarity of the power
228 supply the sense of the skew dipole will change too. To change the sense of
229 only one of the fields, say the normal field only, the wiring of the coils has to
230 change.

231 *6.4. Normal and skew dipoles of variable strength and sense*

232 This subsection describes two ways of generating normal and skew fields
233 of variable strength and sense.

234 *6.4.1. Normal and skew dipoles two independent power supplies*

235 Fig. 19 is schematic diagram showing the wire connection of the coils
236 with two independent power supplies. Such a connection allows independent
237 variation of the normal and skew dipole strength, as well as independent
238 variation of the sense of the dipole fields by changing the polarity of the
239 power supplies.

240 *6.4.2. Normal and skew dipoles with two power supplies one floating*

241 In applications where both normal and skew dipole fields are to maintain
242 almost the same strength a floating power supply maybe used to vary slightly
243 the strength of one of the fields. Fig. 20 is a schematic diagram for the wire
244 connection of the coils of the WF magnet which generates both normal and
245 skew dipoles but of variable strengths between the normal and the skew
246 dipoles. The coils which generate the normal dipole field do not have to be
247 identical to those which generate the skew dipole field. Note that there is
248 an additional power supply which floating. This floating power supply works
249 in conjunction with the regular power supply to adjust the strength and the
250 sense of the normal and skew dipoles independently.

251 *6.5. Normal quadrupole*

252 Fig. 21 is a schematic diagram for the connections of the four identical
253 coils of the WF magnet to generate a normal quadrupole. If the vertical coils
254 are not identical with the horizontal ones the strength of the quadrupole will
255 correspond to the the coils with the least ampere-turns.

256 *6.6. Combination of Normal Quadrupole and Normal or Skew Dipole*

257 This can be accomplished in two ways as it is described in the following
258 two subsections below.

259 *6.6.1. Separate Quad and Dipole coils powered by separate power supplies*

260 Fig. 22 is a schematic diagram for the connections of the Quadrupole coils
261 (4 coils) by a power supply and the connection of the Dipole coils (2 coils) by
262 a separate power supply. This method requires six racetrack coils and two
263 power supplies.

264 *6.6.2. Using floating power supplies to generate Normal Quad and Normal
265 of Skew Dipole*

266 *6.7. Combination of Normal Quadrupole with Normal and Skew Dipole*

267 This can be accomplished in two ways as it is described in the following
268 two subsections below.

269 *6.7.1. Normal Quad Normal Dipole and Skew Dipole*

270 The Quad-coils, the Normal-Dipole-coils and the Skew-Dipole-coils are
271 all separate and each type of coils is powered by a separate power supply.
272 In all this method requires 8 coils and three power supplies. To reduce the
273 sextupole component generated by the dipole coils it is recommended to
274 wound the dipole coils right up against the iron frame.

275 *6.7.2. Normal Quad Normal Dipole and Skew Dipole with floating PS*

276 Fig. 24 is a schematic diagram for the wire connections of four coils and six
277 power supplies to generate a Normal quadrupole combined with a Normal
278 and Skew dipole field. This method requires four racetrack coils and six
279 power supplies.

280 **7. References**

281 [1] ICFA BD Newsletter No. 74 <http://icfa-bd.kek.jp/>

282 [2] <https://operafea.com/>

283 [3] J. Animesh private communication



Figure 5: A picture of the quadrupole permanent magnet wedges surrounded by the Al cooling block. The coils of the dipole corrector magnet are also shown.

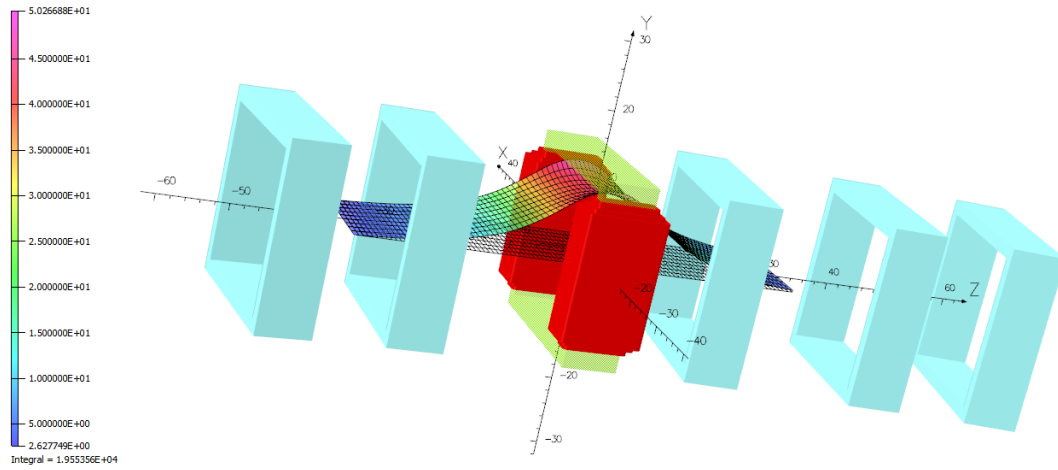


Figure 6: A perspective view of the B_y field on a rectangular patch. The iron of the neighboring window frame magnets appear in the drawing to show the extend the field of a single corrector inside the neighboring magnets. The current in the wire of the coil of the single corrector magnet is at its maximum value of 2.29 A.

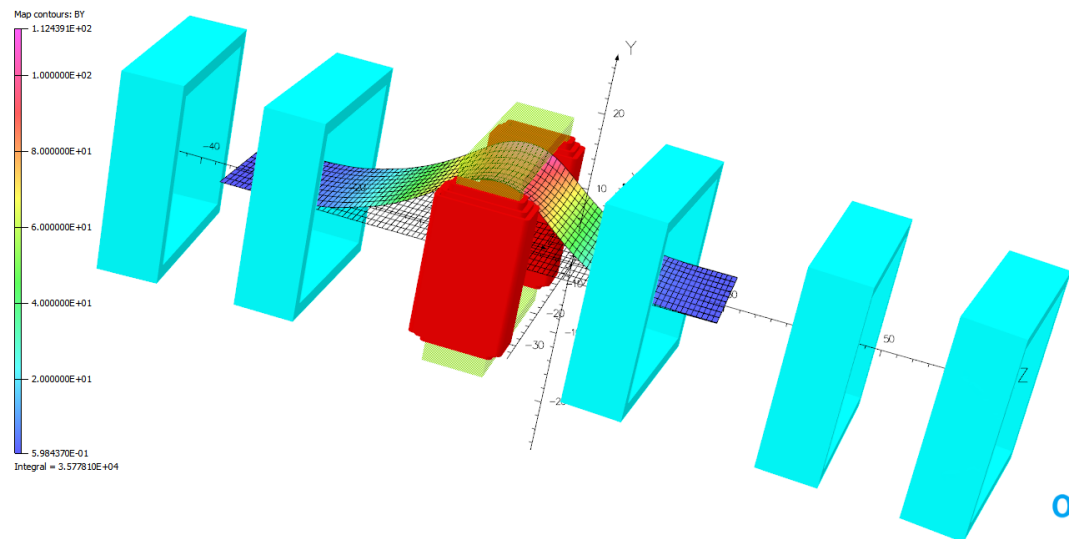


Figure 7: A perspective view of the B_y field on a rectangular patch. The iron of the neighboring window frame magnets appear in the drawing to show the extend the field of a single corrector inside the neighboring magnets. The current in the wire of the coil of the single corrector magnet is at its maximum value of 2.29 A. The extend of the field of the corrector magnet with the coils is reduced when the material of the neighboring iron frames has the same permeability as the iron of the corrector magnet with the coils.

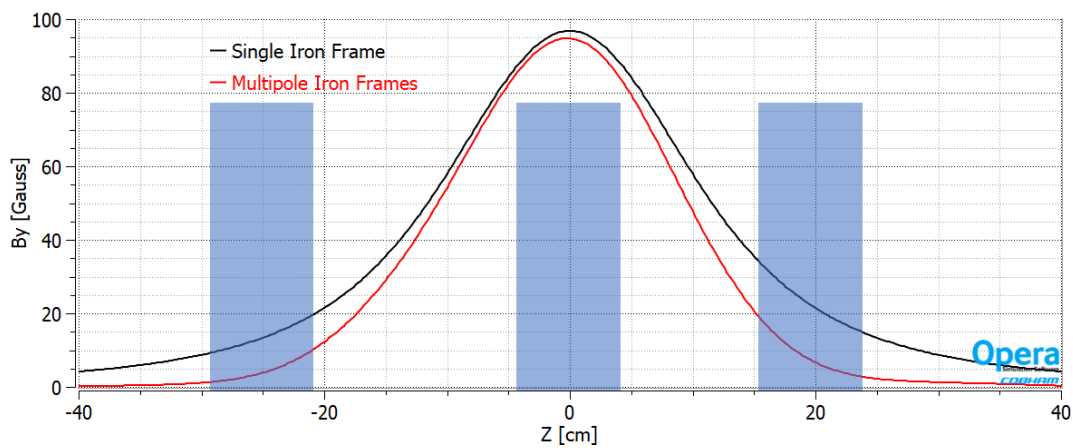


Figure 8: The B_y component of the field as a function of z distance measured from the center of the corrector magnet. The rectangles on the figure are the iron frames of the corrector magnets. The black curve corresponds to the B_y field with all the window frames having permeability $\mu=1$ except the window frame which generates the field and has the permeability of magnetic iron. The red curve corresponds to the B_y field with all the window frames having permeability of iron. Notice the red curve is not symmetric with respect to the center of the magnet because the neighboring iron frames are not placed symmetrically to the central one.

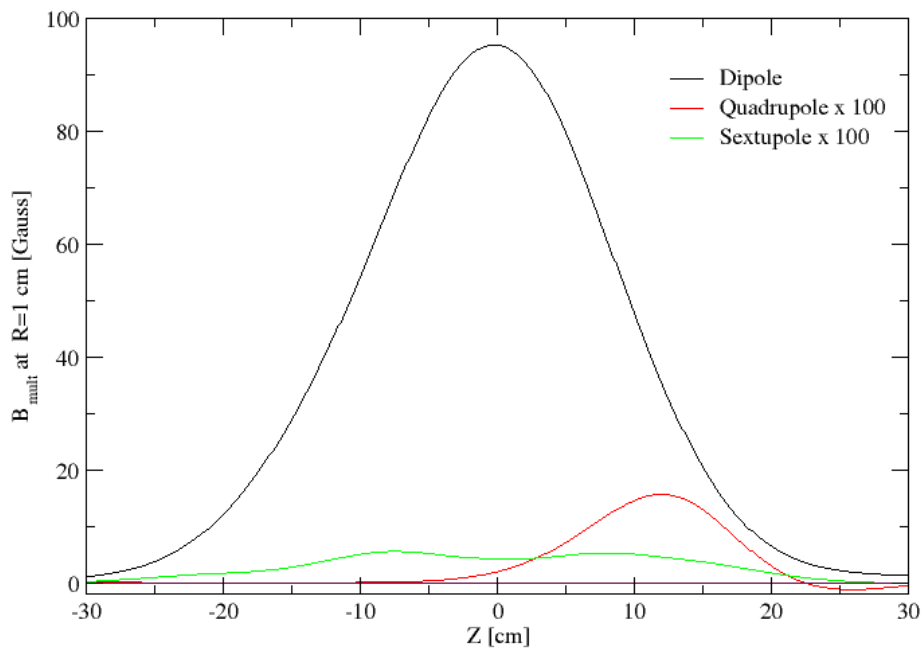


Figure 9: The dipole, quadrupole and sextupole multipoles as a function of the longitudinal distance z . The multipoles are the Fourier expansion of the radial field at a radius $R=1$ cm. Notice that the values of the quadrupole and sextupole multipoles have been multiplied by 100 to be visible in the graph.

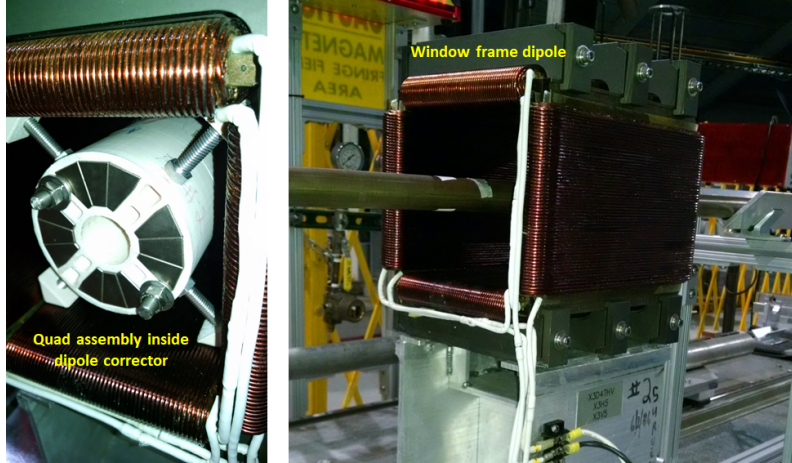


Figure 10: (Left) The window frame dipole magnet surrounding the permanent Halbach type magnet. (Right) An expanded view of the window frame magnet. The cylindrical pipe through the dipole magnet is the rotating coil which measures the integrated multipoles of the PM-Quad+WF-Dipole assembly.

Effect of Window Frame Yoke Only

Normal Terms:		B_ref = 0.037748 T.m (at R_ref = 10 mm)				
Harmonic Number	PMQ Only	PMQ + WF (0A)	Normalized to B_ref (in "units" of 1E-4)			
	In T.m	In T.m	PMQ Only	PMQ + WF (0A)	Change	
1	-2.605E-10	-4.721E-11	0.00	0.00	0.00	
2	3.775E-02	3.796E-02	10000.00	10055.85	55.85	
3	-5.700E-06	-6.980E-06	-1.51	-1.85	-0.34	
4	-4.375E-06	2.328E-06	-1.16	0.62	1.78	
5	-6.699E-06	-5.863E-06	-1.77	-1.55	0.22	
6	-7.103E-04	-7.115E-04	-188.17	-188.49	-0.33	
7	-1.986E-06	-2.011E-06	-0.53	-0.53	-0.01	
8	-1.352E-06	-1.006E-06	-0.36	-0.27	0.09	
9	3.260E-07	2.609E-07	0.09	0.07	-0.02	
10	-9.706E-06	-9.733E-06	-2.57	-2.58	-0.01	
11	1.039E-07	1.258E-07	0.03	0.03	0.01	
12	8.371E-08	3.132E-08	0.02	0.01	-0.01	
13	-2.289E-08	-1.424E-08	-0.01	0.00	0.00	
14	4.206E-07	4.127E-07	0.11	0.11	0.00	
15	-8.415E-10	-2.036E-09	0.00	0.00	0.00	

Effect of Window Frame Yoke Only

Skew Terms:		B_ref = 0.037748 T.m (at R_ref = 10 mm)				
Harmonic Number	PMQ Only	PMQ + WF (0A)	Normalized to B_ref (in "units" of 1E-4)			
	In T.m	In T.m	PMQ Only	PMQ + WF (0A)	Change	
1	9.605E-11	2.870E-11	0.00	0.00	0.00	
2	-1.379E-11	7.030E-12	0.00	0.00	0.00	
3	-3.337E-05	-3.500E-05	-8.84	-9.27	-0.43	
4	-9.634E-06	-1.032E-05	-2.55	-2.73	-0.18	
5	-2.898E-05	-1.477E-05	-7.68	-3.91	3.76	
6	-6.135E-06	-6.495E-06	-1.63	-1.72	-0.10	
7	4.046E-06	4.053E-06	1.07	1.07	0.00	
8	-3.741E-07	-3.879E-07	-0.10	-0.10	0.00	
9	2.946E-07	3.704E-07	0.08	0.10	0.02	
10	1.982E-08	-5.434E-10	0.01	0.00	-0.01	
11	3.545E-08	4.723E-08	0.01	0.01	0.00	
12	7.834E-10	4.462E-09	0.00	0.00	0.00	
13	1.323E-08	7.317E-09	0.00	0.00	0.00	
14	-1.898E-09	-1.110E-08	0.00	0.00	0.00	
15	-1.086E-08	-3.017E-09	0.00	0.00	0.00	

Figure 11: The effect of the WF yoke on the integrated normal (left) and skew (right) multipoles of the PM quadrupole.

Superposition for Horizontal Field Dipole

Superposition for Horizontal Field Dipole

Normal Terms: B_ref used for Normalization= 0.037959 T.m (at Reference radius = 10 mm)								Skew Terms: B_ref used for Normalization= 0.037959 T.m (at Reference radius = 10 mm)							
Harmonic Number	PMQ + WF (0A)	SKD Only (10A)	PMQ + SKD (10A)	Normalized to B_ref (in "units" of 1E-4)				Harmonic Number	PMQ + WF (0A)	SKD Only (10A)	PMQ + SKD (10A)	Normalized to B_ref (in "units" of 1E-4)			
	in T.m	in T.m	in T.m	PMQ+WF(0A)	SKD Only (10A)	PMQ+SKD (10A)	Superposition Error		in T.m	in T.m	in T.m	PMQ+WF(0A)	SKD Only (10A)	PMQ+SKD (10A)	Superposition Error
1	-4.721E-11	-4.322E-05	-6.223E-05	0.00	-11.39	-16.39	5.01	1	2.870E-11	5.680E-03	5.658E-03	0.00	1496.37	1490.51	5.86
2	3.796E-02	3.662E-06	3.795E-02	10000.00	0.96	9998.02	2.95	2	7.030E-12	3.259E-06	-8.500E-07	0.00	0.86	-0.22	1.08
3	-6.980E-06	-1.976E-07	-6.775E-06	-1.84	-0.05	-1.78	-0.11	3	-3.500E-05	-7.188E-06	-5.042E-05	-9.22	-1.89	-13.28	2.17
4	2.328E-06	-3.922E-08	1.859E-06	0.61	-0.01	0.49	0.11	4	-1.032E-05	-1.644E-08	-1.011E-05	-2.72	0.00	-2.66	-0.06
5	-5.863E-06	7.459E-09	-5.499E-06	-1.54	0.00	-1.45	-0.09	5	-1.477E-05	7.578E-08	-9.787E-06	-3.89	0.02	-2.58	-1.29
6	-7.115E-04	-7.467E-09	-7.119E-04	-187.45	0.00	-187.55	0.10	6	-6.495E-06	2.810E-09	-6.614E-06	-1.71	0.00	-1.74	0.03
7	-2.011E-06	-2.511E-09	-2.085E-06	-0.53	0.00	-0.55	0.02	7	4.053E-06	-6.512E-09	3.933E-06	1.07	0.00	1.04	0.03
8	-1.006E-06	4.542E-09	-1.024E-06	-0.26	0.00	-0.27	0.01	8	-3.879E-07	-1.089E-09	-3.807E-07	-0.10	0.00	-0.10	0.00
9	2.609E-07	8.358E-10	2.591E-07	0.07	0.00	0.07	0.00	9	3.704E-07	2.525E-09	3.954E-07	0.10	0.00	0.10	-0.01
10	-9.733E-06	-1.582E-09	-9.732E-06	-2.56	0.00	-2.56	0.00	10	-5.434E-10	9.721E-10	-6.038E-09	0.00	0.00	0.00	0.00
11	1.258E-07	-4.136E-10	1.251E-07	0.03	0.00	0.03	0.00	11	4.723E-08	-8.825E-10	3.787E-08	0.01	0.00	0.01	0.00
12	3.132E-08	7.563E-10	3.366E-08	0.01	0.00	0.01	0.00	12	4.462E-09	6.928E-13	1.388E-08	0.00	0.00	0.00	0.00
13	-1.424E-08	-1.432E-11	-1.159E-08	0.00	0.00	0.00	0.00	13	7.317E-09	1.955E-10	6.069E-09	0.00	0.00	0.00	0.00
14	4.127E-07	-3.192E-10	4.146E-07	0.11	0.00	0.11	0.00	14	-1.110E-08	-7.127E-11	-9.620E-09	0.00	0.00	0.00	0.00
15	-2.036E-09	-3.192E-11	-4.322E-09	0.00	0.00	0.00	0.00	15	-3.017E-09	-5.052E-10	-2.756E-09	0.00	0.00	0.00	0.00

Figure 12: The effect of the Horizontal field generated by the WF dipole magnet which is excited at its nominal current on the integrated normal (left) and skew (right) multipoles of the PM quadrupole.

Superposition for Vertical Field Dipole

Superposition for Vertical Field Dipole

Normal Terms: B_ref used for Normalization= 0.037959 T.m (at Reference radius = 10 mm)								Skew Terms: B_ref used for Normalization= 0.037959 T.m (at Reference radius = 10 mm)							
Harmonic Number	PMQ + WF (0A)	NSD Only (10A)	PMQ + NSD (10A)	Normalized to B_ref (in "units" of 1E-4)				Harmonic Number	PMQ + WF (0A)	NSD Only (10A)	PMQ + NSD (10A)	Normalized to B_ref (in "units" of 1E-4)			
	in T.m	in T.m	in T.m	PMQ+WF(0A)	NSD Only (10A)	PMQ+NSD (10A)	Superposition Error		in T.m	in T.m	in T.m	PMQ+WF(0A)	NSD Only (10A)	PMQ+NSD (10A)	Superposition Error
1	-4.721E-11	5.725E-03	5.685E-03	0.00	1508.27	1497.69	10.59	1	2.870E-11	-5.418E-06	-4.744E-05	0.00	-1.43	-12.50	11.07
2	3.796E-02	-1.402E-06	3.791E-02	10000.00	-0.37	9987.18	12.45	2	7.030E-12	3.439E-06	-4.819E-06	0.00	0.91	-1.27	2.18
3	-6.980E-06	7.155E-06	9.719E-06	-1.84	1.88	2.56	-2.51	3	-3.500E-05	-1.950E-07	-3.480E-05	-9.22	-0.05	-9.17	-0.10
4	2.328E-06	-2.784E-09	1.932E-06	0.61	0.00	0.51	0.10	4	-1.032E-05	4.866E-08	-9.881E-06	-2.72	0.01	-2.60	-0.10
5	-5.863E-06	6.489E-08	-6.789E-07	-1.54	0.02	-0.18	-1.35	5	-1.477E-05	1.669E-08	-5.127E-06	-3.89	0.00	-1.35	-2.54
6	-7.115E-04	-5.749E-09	-7.120E-04	-187.45	0.00	-187.56	0.12	6	-6.495E-06	3.208E-09	-6.636E-06	-1.71	0.00	-1.75	0.04
7	-2.011E-06	-3.712E-09	-1.783E-06	-0.53	0.00	-0.47	-0.06	7	4.053E-06	-6.325E-09	4.095E-06	1.07	0.00	1.08	-0.01
8	-1.006E-06	4.475E-09	-1.007E-06	-0.26	0.00	-0.27	0.00	8	-3.879E-07	-7.565E-10	-3.980E-07	-0.10	0.00	-0.10	0.00
9	2.609E-07	4.326E-10	2.720E-07	0.07	0.00	0.07	0.00	9	3.704E-07	2.941E-09	5.991E-07	0.10	0.00	0.16	-0.06
10	-9.733E-06	-1.647E-09	-9.710E-06	-2.56	0.00	-2.56	-0.01	10	-5.434E-10	4.014E-10	1.228E-09	0.00	0.00	0.00	0.00
11	1.258E-07	-6.315E-10	9.174E-08	0.03	0.00	0.02	0.01	11	4.723E-08	-3.895E-10	4.418E-08	0.01	0.00	0.01	0.00
12	3.132E-08	8.695E-10	4.591E-08	0.01	0.00	0.01	0.00	12	4.462E-09	-2.470E-10	6.559E-09	0.00	0.00	0.00	0.00
13	-1.424E-08	-3.212E-11	-1.465E-08	0.00	0.00	0.00	0.00	13	7.317E-09	4.730E-10	-1.156E-09	0.00	0.00	0.00	0.00
14	4.127E-07	-2.452E-10	4.154E-07	0.11	0.00	0.11	0.00	14	-1.110E-08	-8.983E-11	-8.974E-09	0.00	0.00	0.00	0.00
15	-2.036E-09	-4.463E-11	-7.737E-10	0.00	0.00	0.00	0.00	15	-3.017E-09	-2.019E-10	-2.024E-09	0.00	0.00	0.00	0.00

Figure 13: The effect of the Vertical field generated by the WF dipole magnet on the integrated normal (left) and skew (right) multipoles of the PM quadrupole.

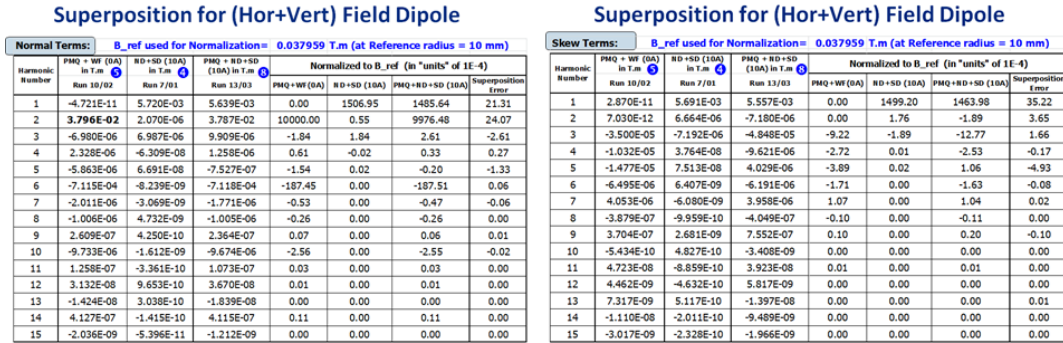


Figure 14: The effect of the Horizontal and Vertical fields generated by the WF dipole magnet on the integrated normal (left) and skew (right) multipoles of the PM quadrupole.

Summary

- Field superposition was tested for a permanent magnet quadrupole in horizontal and vertical dipole fields of ~20 mT each.
- Presence of iron yoke of the window frame dipole enhances the quadrupole field by ~ 0.5%.
- Use of a 1 m long rotating coil causes some error in the analysis due to double counting of background fields.
- For higher harmonics, the deviation from a perfect superposition is less than 5 units (0.05% of the quadrupole field) at a reference radius of 10 mm.
- Error in the dipole and quadrupole terms can be much more, up to ~30 units (normalized to quadrupole field.)

Figure 15: The summary of the measurements as provided by [3]

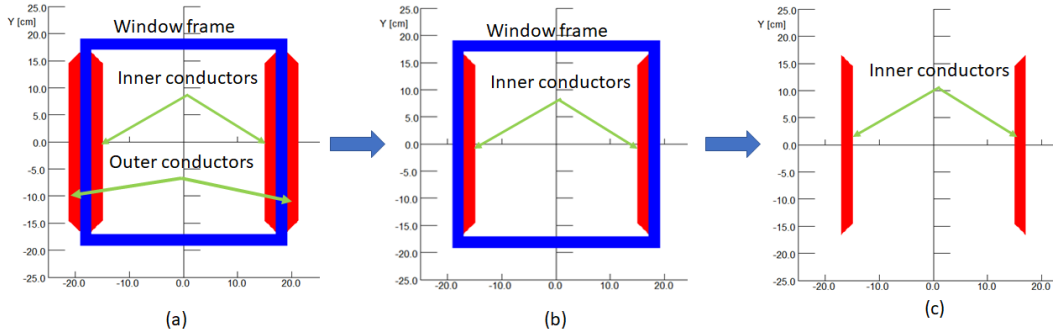


Figure 16: The cross section of a WF magnet (a) with two racetrack coils wound around the vertical sides of the frame to generate normal dipole field. In this appendix this magnet will be represented by the two inner conductors of the coil as shown in (c).

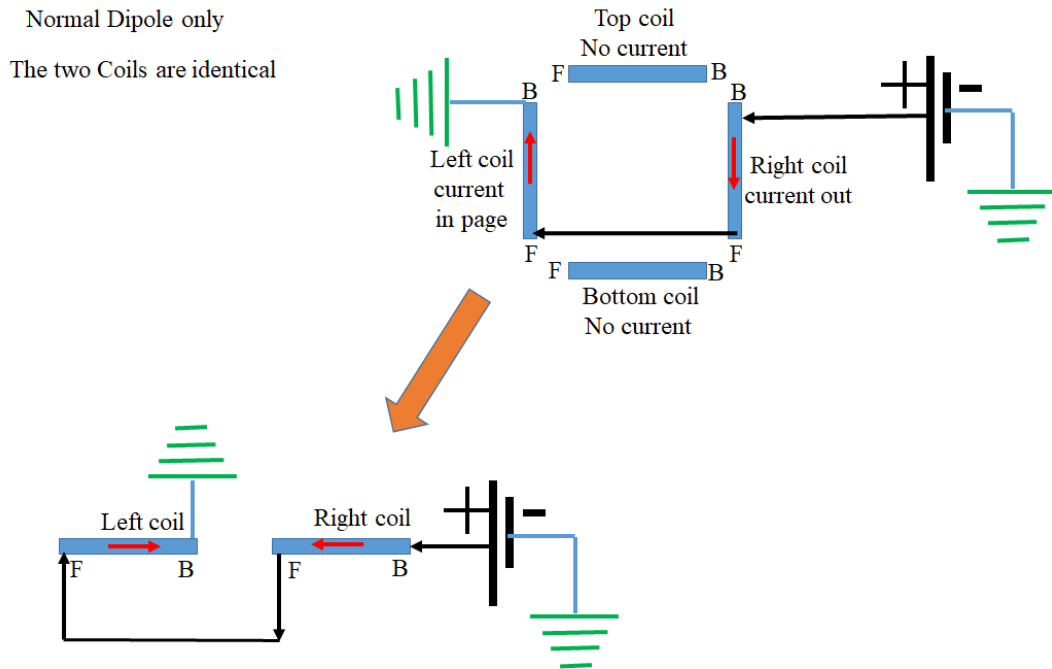


Figure 17: A schematic diagram showing the connection of the coils to generate a normal dipole field. Note that the top and bottom coils are not connected to a power supply.

Normal + Skew Dipole
 Same strength
 All four Coils are identical

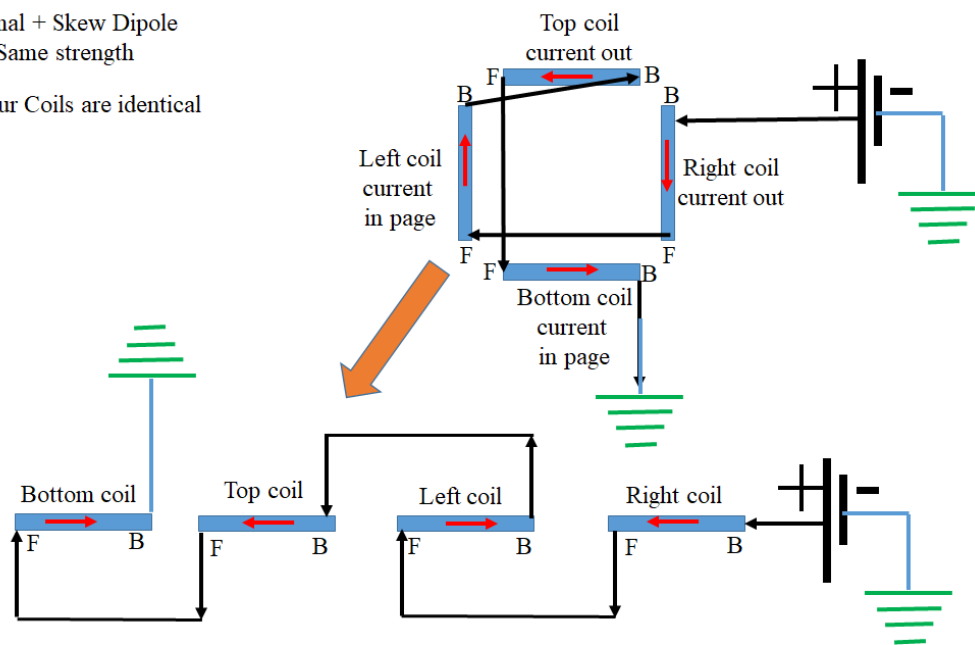


Figure 18: A schematic diagram showing the connection of the coils to generate simultaneous a normal and skew dipole field. If the coils which generate normal field are identical to those which generate vertical field the strength of the dipoles is the same.

Normal + Skew Dipole
 Variable strength and sense
 Independent power supplies

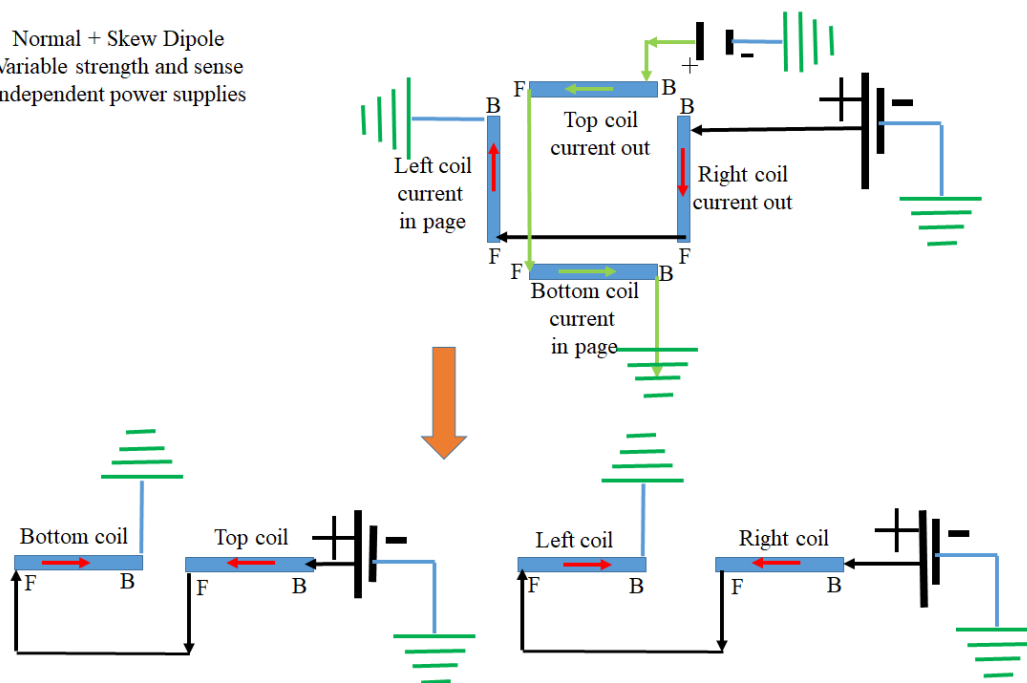


Figure 19: A schematic diagram showing the wire connection of the coils with two independent power supplies. Such a connection allows independent variation of the normal and skew dipole strength, as well as independent variation of the sense of the dipole fields by changing the polarity of the power supplies.

Normal + Skew Dipole
Variable strength

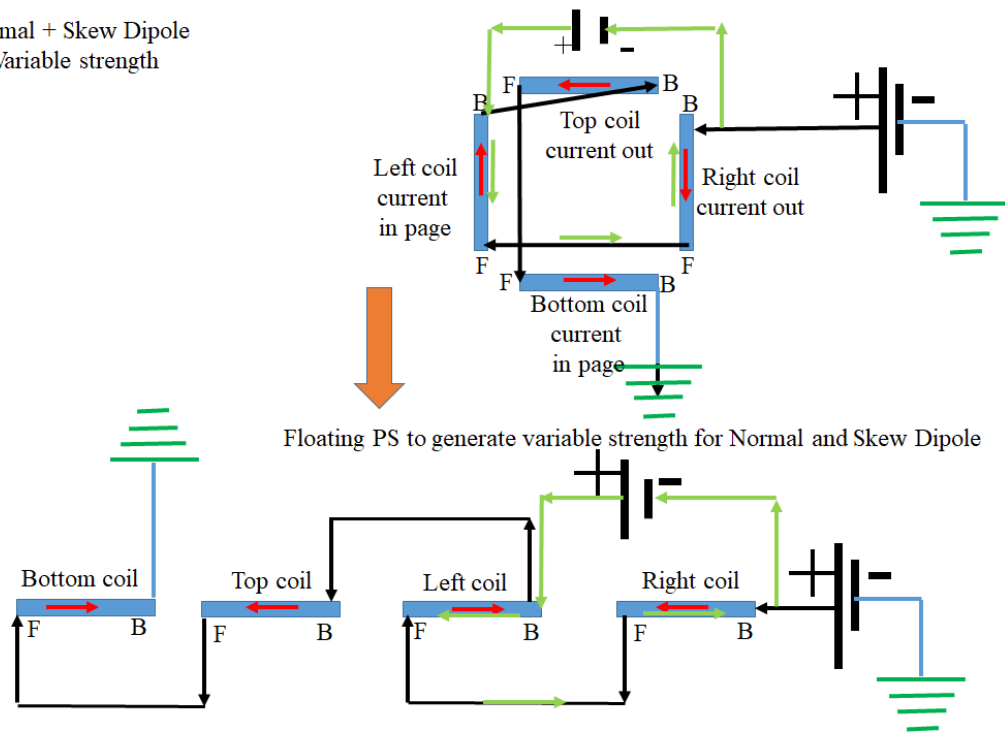


Figure 20: A schematic diagram for the wire connection of the coils of the WF magnet which generates both normal and skew dipoles but of variable strengths between the normal and the skew dipoles. The coils which generate the normal dipole field do not have to be identical to those which generate the skew dipole field.

Normal Quadrupole
 All four Coils are identical
 Normal Quadrupole

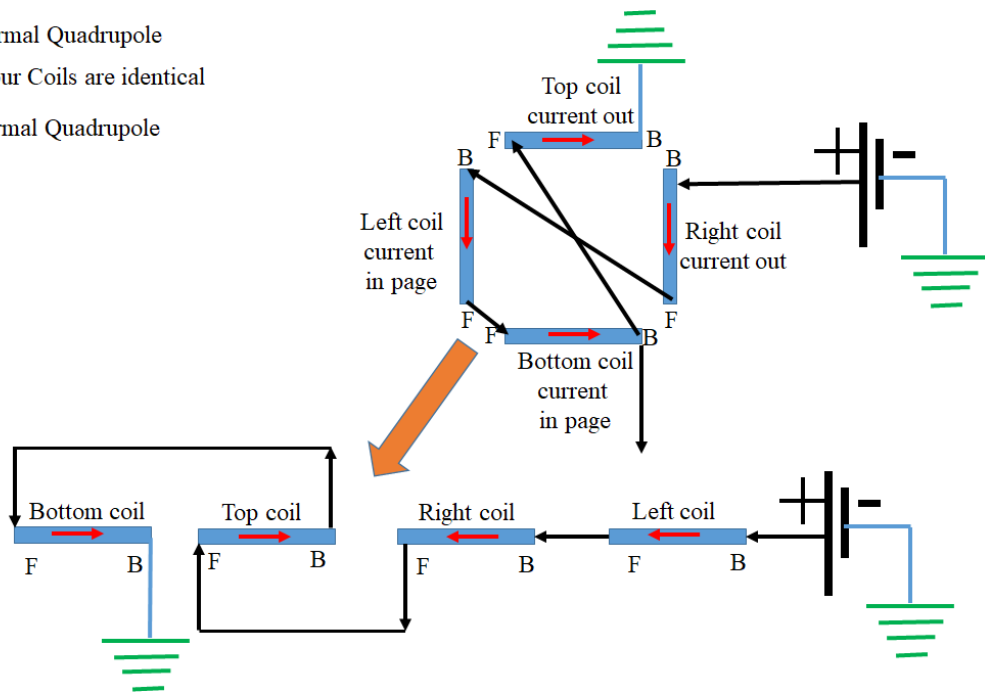


Figure 21: A schematic diagram for the connections of the four identical coils of the WF magnet to generate a normal quadrupole. If the vertical coils are not identical with the horizontal ones the strength of the quadrupole will correspond to the the coils with the least ampere-turns.

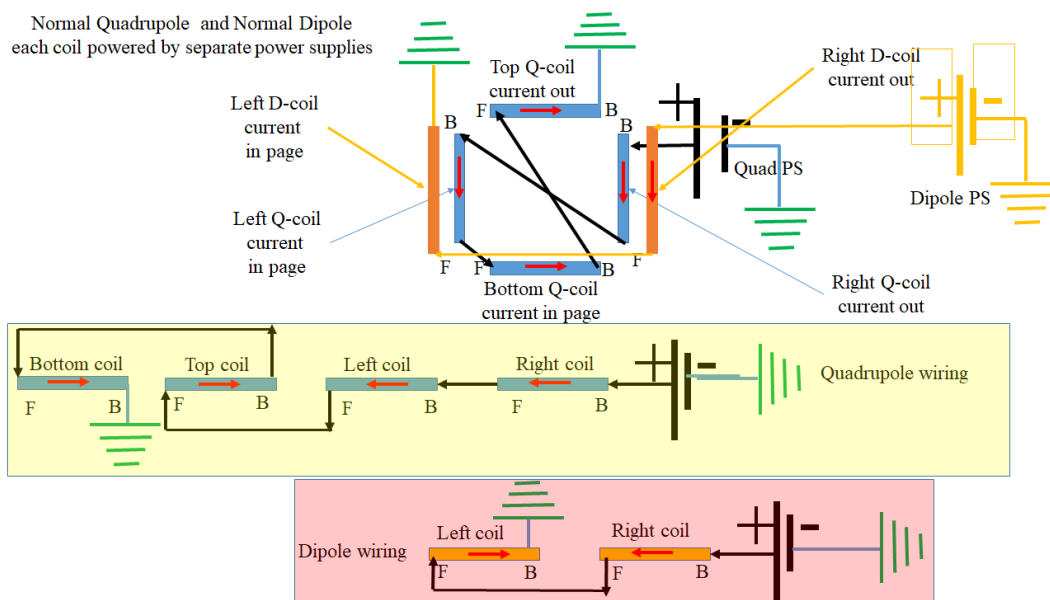


Figure 22: A schematic diagram for the connections of the Quadrupole coils by a power supply and the connection of the Dipole coils by a separate power supply. This method requires six racetrack coils and two power supplies.

Normal Quadrupole + Normal Dipole
 All four Coils are identical

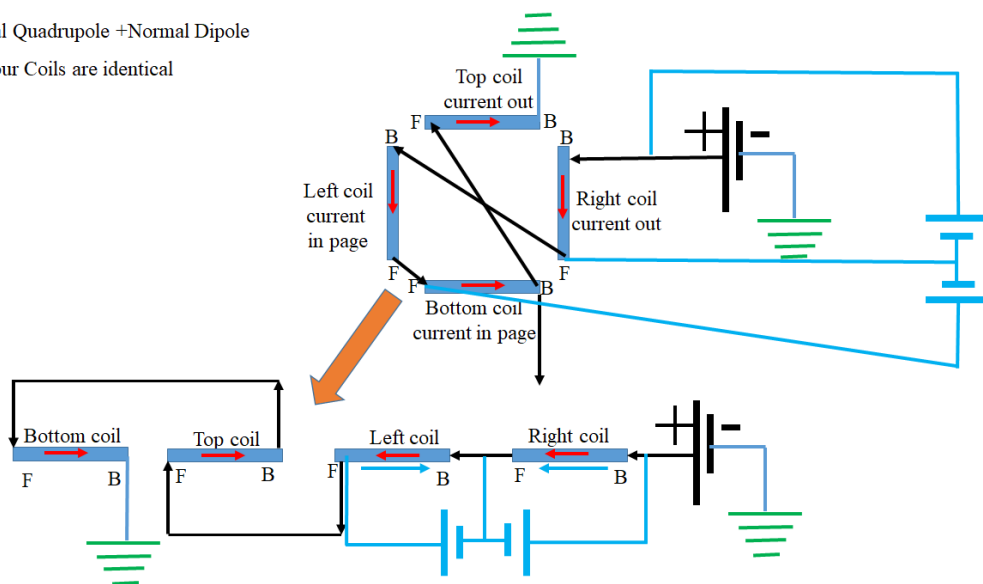


Figure 23: A schematic diagram of wiring four coils with three power supplies (two PS floating) to generate a combined quadrupole and dipole field. This method requires four coils and three power supplies.

Normal-Quadrupole + Normal and Skew Dipoles
 All four Coils are identical

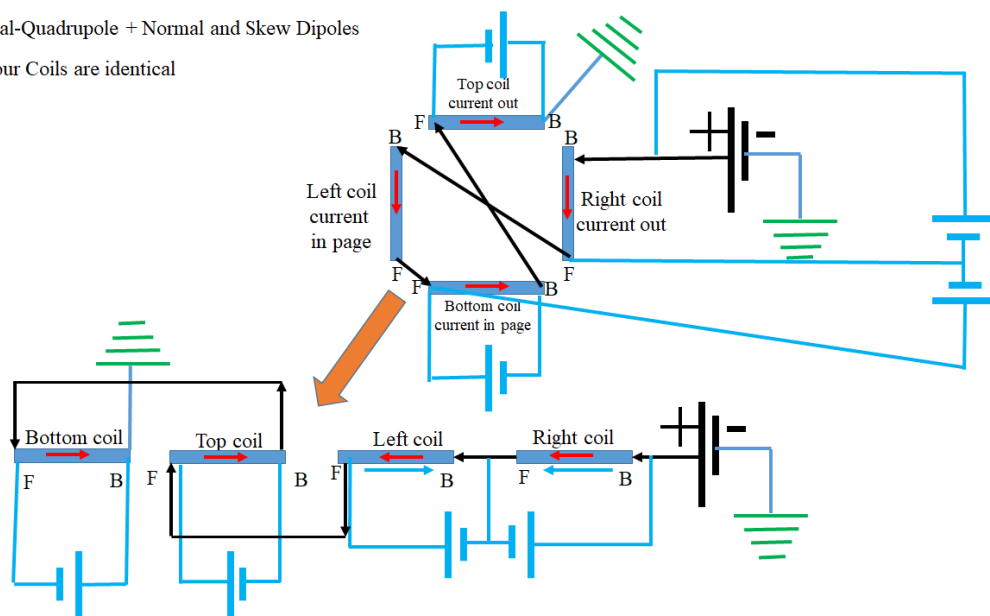


Figure 24: A schematic diagram of wiring four coils with five power supplies (4 PS are floating) to generate a Normal quadrupole combined with a Normal and Skew dipole field. This method requires four coils and six power supplies.